We are IntechOpen,
the world's leading publisher of
Open Access books
Built by scientists, for scientists

6,900
Open access books available

186,000
International authors and editors

200M
Downloads

Our authors are among the

154
Countries delivered to

TOP 1%
most cited scientists

12.2%
Contributors from top 500 universities

Interested in publishing with us?
Contact book.department@intechopen.com

Numbers displayed above are based on latest data collected.
For more information visit www.intechopen.com

Investigation of Optical Properties and Radiation Stability of TiO$_2$ Powders before and after Modification by Nanopowders of Various Oxides

Mikhail M. Mikhailov, Vitaly V. Neshchimenko,
Semyon A. Yuryev and Alexey N. Sokolovskiy

Additional information is available at the end of the chapter

Abstract

The titanium dioxide powders are widely used as a pigment for coatings and paints, the important characteristics of which are reflectivity and stability to irradiation. The results of investigations of the optical properties and radiation stability of titanium dioxide powders before and after high-temperature modification with nanopowders are presented in this chapter. The diffuse reflection spectra of various titanium dioxide powders in the UV, visible, and near-IR ranges, and their change during irradiation by electrons with 30 keV energy and a different fluence in vacuum *in situ* were investigated: (1) TiO$_2$ powders with particle size in the range 60–240 nm; (2) Microsized TiO$_2$ powder (240 nm) modified by Al$_2$O$_3$, ZrO$_2$, SiO$_2$, TiO$_2$, ZnO, MgO nanoparticles with grain size from 30 up to 60 nm; (3) Microsized TiO$_2$ powder (260 nm) modified by SiO$_2$ with the grain size of 12–14 nm at the temperature of 150, 400, and 800°C. The reduction in reflectivity in entire spectrum with decrease in grain sizes of TiO$_2$ nanopowders was established. Nanopowder with the grain size of 80 nm possesses the highest stability to irradiation. It was shown that the average grain size and specific surface of introduced nanoparticles effect noticeably on the radiation stability increase of titanium dioxide powders modified with nanoparticles of various oxides. The micro-sized TiO$_2$ powder heating at temperature of 800°C is the factor which positively influences on the radiation stability.

Keywords: titanium dioxide, nanoparticles, optical properties, radiation stability, modification, irradiation, defects

1. Introduction

The titanium dioxide powders are widely used in many branches of industry. They are utilized as effective photocatalyst [1–3], pigments of thermal control, and anti-reflective coatings of spacecraft [4, 5]. In recent years, the investigations of possibility of their usage as solar photoconverters are conducted [6, 7]. But they have found the largest application as household paints [8].

Such fields of the use imply a work in conditions of an action of charged particle fluxes, UV, and visible radiations. The absorption centers, caused by cation and anion defect sublattices, are formed due to these radiations. That is why the method development of an increase in radiation stability of titanium dioxide powders is a relevant problem.

Theoretical and experimental studies revealed [9–14] that the modification with nanopowders is sufficiently effective way to increase the radiation stability because they possess large specific surface and work as a "sink" for gathering electronic excitations formed during irradiation. However, the modification by nanopowders can lead to a deterioration of initial optical properties that can be induced by large absorption of native point defects in the UV and visible ranges and by absorption of chemosorbed gases in near-infrared (IR) range of spectrum. The modification is associated with high temperature heating of powders, an effect of which on optical properties and radiation stability is studied poorly.

An influence of the modification by nanopowders on photo- and radiation stability of reflective powders is discussed in [9–14]. There are no data about an effect of modification conditions (temperature and heating time, type, and concentration of nanopowders) on the optical properties of materials and their stability to an impact of ionizing radiations.

In the present chapter, the data obtained by the authors regarding optical properties and radiation stability of titanium dioxide powders before and after modification with nanoparticles of various oxides are considered. The radiation stability of titanium dioxide powders of different sizes and different types of crystal structures is considered. The results of investigations of the rutile titanium dioxide powder modification by nanoparticles of oxide compounds at the temperature of 800°C as well as the studies of an effect of the anatase titanium dioxide powder modification by SiO_2 nanoparticles with large specific surface at the temperatures of 150, 400, and 800°C are presented.

2. Experimental

For modification by various nanoparticles, the rutile TiO_2 powders with the average particle size of 240 nm and specific surface of 8 m^2/g were used. The anatase TiO_2 powders with the average particle size of 260 nm and specific surface of 7 m^2/g were used for modification with SiO_2 nanoparticles (average particle size 12–14 nm). The TiO_2 powder was mixed with oxide nanoparticles in a ratio 100:7, the distilled water was added, and it was evaporated at the temperature of 150°C for 6 hours. Then, the mixture was heated in an oven for 2 hours at 400 or 800°C. After heating, the mixture was grinded in agate mortar and was pressed into metal substrates with 28 mm diameter and 2 mm height. The prepared samples were mounted in

space environment simulator "Spektr" [15]. Since the sample interaction with atmospheric oxygen after irradiation can lead to "bleaching"—a decrease in concentration of formed absorption centers of oxide reflective powders, the diffuse reflection spectra (ρ_λ) were registered in vacuum (*in situ*) after irradiation with accelerated electrons (E = 30 keV, φ = $1 \cdot 10^{12}$ cm^{-2} s^{-1}, F = (0.5, 1, and 2) × 10^{16} cm^{-2}, T = 300 K, P = 10^{-6} torr). The radiation stability was evaluated with using the difference spectra and the change in integral absorption coefficient of solar radiation (a_s), which is computed from diffuse reflection spectra according to the following expression:

$$a_s = 1 - R_s = 1 - \frac{\int_{\lambda_1}^{\lambda_2} \rho_\lambda I_\lambda d\lambda}{\int_{\lambda_1}^{\lambda_2} I_\lambda d\lambda} = 1 - \frac{\sum_{i=1}^{n} \rho_\lambda}{n},$$ (1)

where ρ_λ—spectral reflectivity; I_λ—solar radiation intensity; $\lambda_1 \div \lambda_2$—Sun spectrum range (the Sun radiates 98% of total energy in the range of 0.2 ÷ 2.5 µm); n—the number of equienergy ranges of the solar spectrum [16].

Changes in absorption coefficient a_s were defined from subtraction its values before (a_{s0}) and after ($a_{s,irr}$) irradiation of powders by accelerated electrons:

$$\Delta a_s = a_{s,irr} - a_{s0}$$ (2)

3. Optical properties and radiation stability of micro and nanopowders of titanium dioxide before modification

The study objects were the TiO₂ submicron sized powders of industry production with an average particle size of 240 nm (m−240), as well as nanopowders with an average particle size of 60 (n−60), 80 (n−80), and 160 (n−160) nm. The specific surface of m−240, n−160, n−80, and n−60 powders was 8.0, 13, 16, and 28 m²/g, respectively [17].

The m−240 powder possessed rutile lattice, and the nanopowders were the mixture of anatase and rutile. The ratio of these phases changed with the change in particle size. With a decrease in particle size from 160 down to 80 and 60 nm, the concentration of rutile changed from 50 down to 33.9 and 98.7 mass%, the anatase concentration was 49.8, 66.1, and 1.3 mass%.

The largest value of the reflection coefficient (ρ_0) was registered in $\rho_{\lambda 0}$ spectra of micropowder m−240. The nanopowders n−160, n−80, and n−60 follow in order of its decrease (**Figure 1**).

The absolute values of the reflection coefficient on the various regions of the spectrum reduce with decreasing powder particle sizes. Its largest values are registered in the range from 500 to 1200 nm. The reflection coefficient reduces in more short-wavelength (λ < 500 nm) and more long-wavelength (λ >1200 nm) ranges. The more is the decrease, the less is the size particles of powders. In the short-wavelength region, the decrease in the reflection coefficient is sharp with pronounced outlines of the absorption bands, and in the long-wavelength region, the decay is
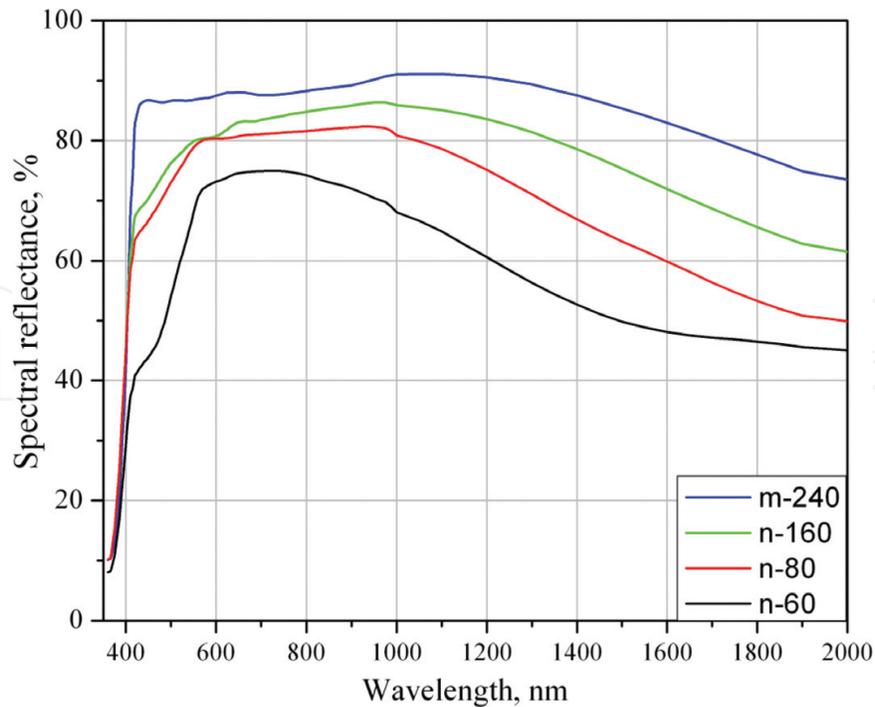
**Figure 1.** The diffuse reflection spectra of TiO₂ powders measured in vacuum (*in situ*).

smooth. The more is the reflection coefficient, the less is the specific surface of the powders in the range of values 8–13 m²/g.

Such a character of the difference in the reflection coefficient on the various regions of the spectrum allows to believe that its reduction is determined by a variety of factors. For their identification, the difference diffuse reflection spectra were obtained by means of subtraction from 100% value of ρ in ρ_{E0} spectra, which depend on energy:

$$\Delta\rho_{E0} = (100 - \rho_{E0}) \tag{3}$$

Such spectra (**Figure 2**) are the absorption spectra of powders before modification. They indicate which absorption bands define a decrease in reflection coefficient. Qualitatively, all spectra are similar. They consist of three regions. First region from absorption edge up to 2.5 eV is characterized by several absorption bands. These bands are encased in integral contour, which is defined by native point defects of titanium dioxide. The intensity of this band in the maximum is 15, 33, 38, and 60%. It is inversely proportional to particle sizes of powders m−240, n−160, n−80, and n−60.

The second region is characterized by an absence of relationship between $\Delta\rho$ and energy. Its length depends on grain size of powders: the less is the grain size, the shorter is the region. The second region of m−240 powder is in the range of 3–1 eV, n−60 powder—in the range of 2.25–1.5 eV, which has an absorption by $Ti_i^{\cdot}$, $O_i^{\prime}$, $V_O^{\cdot}$, and $Ti_i^{\cdot\cdot}$ defects. There is a dependence of $\Delta\rho$ values on particle size of powders: the less is the particle size, the larger is the absorption coefficient. Since nanoparticles possess the large specific surface, the concentration of native lattice defects on their surface is higher than in micropowders, and consequently, the larger concentration of interstitial titanium ions (Ti_i^X) will be in the nanoparticles.
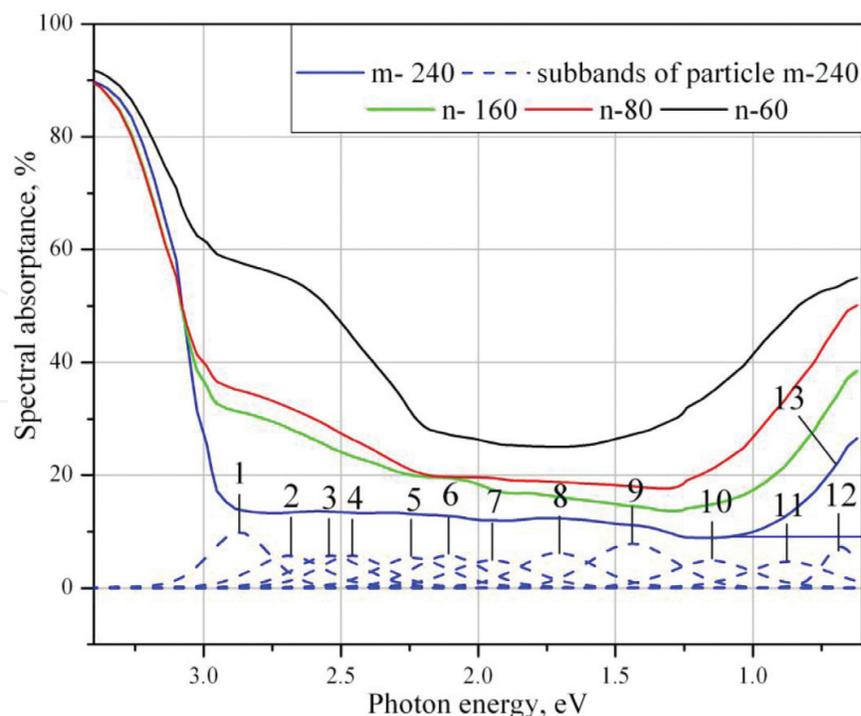
Figure 2. The absorption spectra of the TiO₂ powders before modification: $1-Ti_i^·$, $2-O_i^′$, $3-V_O^·$, $4-Ti_i^{··}$, $5-Ti_i^{···}$, $6-V_O^{··}$, $7-O_i^{″}$, $8-Ti_i^{····}$, $9-V_{Ti}^{″″}$, $10-V_{Ti}^{‴}$, $11-V_O^X$, 12–0.69 eV, 13–free carriers of charge.

The third region in the vicinity above 1.5 eV is determined by increasing values of absorption coefficient with an increase in energy. The slope of these absorption contours is different for various powders: with reducing particle size, the slope increases. In the near-IR range, the absorption of semiconductors is defined by free electrons, which is described by a power law of absorption coefficient from wavelength:

$$\Delta\rho = \eta\lambda^n \tag{4}$$

The power function is defined by free electron transitions between levels in the conductance band. That is why, the exponent can be a measure of free electron concentration [18]. The calculations showed that with the decrease in particle sizes of powders the exponent n increases (**Table 1**). It means that the concentration of free electrons increases with decreasing grain sizes or increasing specific surface.

Thus, the reflection coefficient of initial powders is determined by native point defects and free electrons. The less is the particle sizes of powders, the larger is the concentration of native point defects on the surface and the concentration of free electrons. The particle size defines a value of the reflection coefficient on the first and third regions of the reflection spectra. The

Average particle size of the powders, nm	60	80	160	240
n	1.67	1.53	1.48	0.85

**Table 1.** The dependence of exponent n on the particle sizes of TiO₂ powders.

joint influence of absorption coefficient of point defects and free electrons determines the reflection coefficient in the second region: the larger is the $\Delta\rho$ on the first and third regions, the larger is its value in the second region and the less the size of this region.

Qualitatively, the change in diffuse reflection spectra obtained after irradiation ($\Delta\rho_F$) is the same for all powders (**Figure 3**). They are absorption spectra induced by accelerated electron exposure. The spectra include the bands in the visible range with the maximum at 2.9 eV and wide unstructured band in the near-IR range with maximums at 1 eV.

The $\Delta\rho_{Ea}$ spectra of powders n−60 significantly differ from m−240, n−160, and n−80, where three regions can be distinguished with qualitatively difference of absorption coefficient. The first region is characterized by the presence of absorption bands in UV and visible ranges. The second one has absorption in the range of 2–1.5 eV. The third one is in the range above 1.5 eV with absorption peak in the range of 1–0.7 eV.

In order to understand the origin of bands and to conduct an analysis of nanoparticle size effect on absorption center accumulation, the $\Delta\rho_E$ spectra were decomposed on elementary bands [19–23]. The function of decomposition consists of 80% of Gaussian and 20% of Lorentzian functions [24]. From decomposition of the induced irradiation spectra on absorption spectra, it follows that during electron exposure in m−240, n−160, n−80, and n−60 titanium dioxide
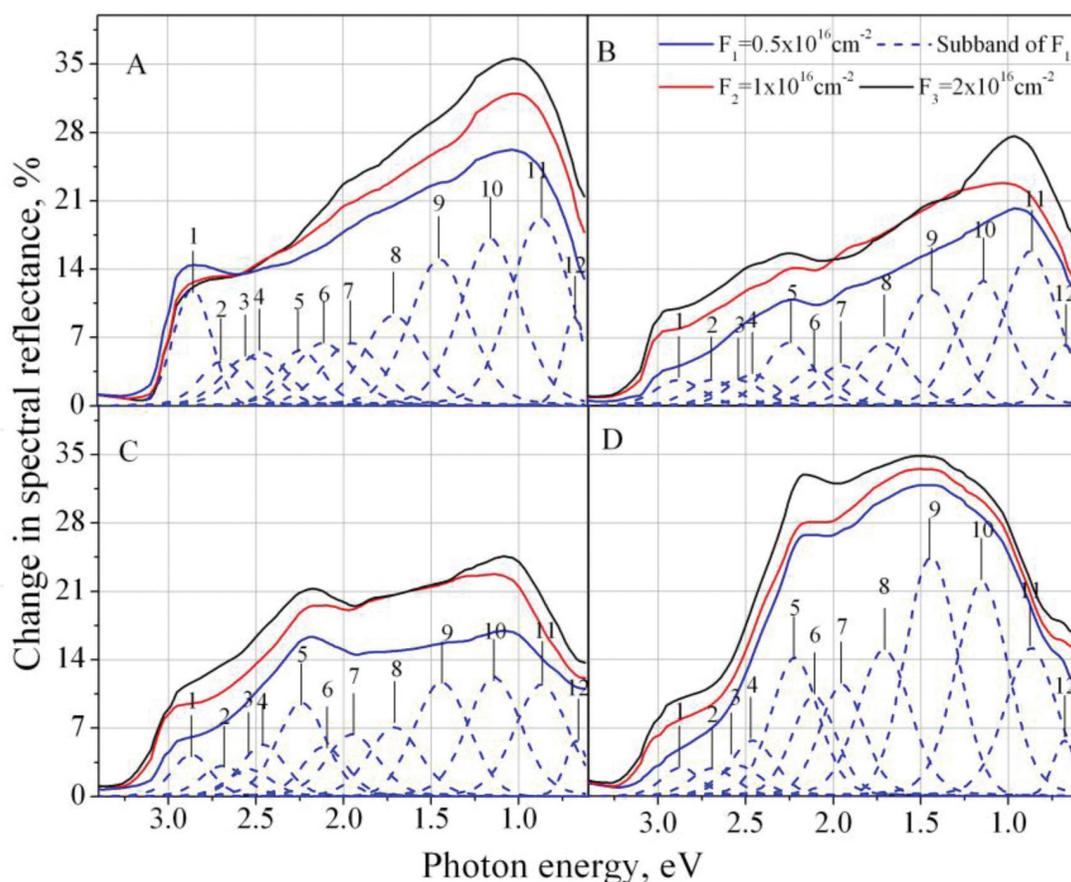
Figure 3. The change in diffuse reflection spectra of titanium dioxide powders m−240 (A), n−160 (B), n−80 (C), and n−60 (D) after electron irradiation with fluence of 0.5 (1), 1 (2), and 2·10^{16} (3) cm^{-2} and after residual vacuum exposure (4). 1−Ti$_i^{\cdot}$, 2−O$_i^{\prime}$, 3−V$_O^{\cdot}$, 4−Ti$_i^{\cdot\cdot}$, 5−Ti$_i^{\cdot\cdot\cdot}$, 6−V$_O^{\cdot\cdot}$, 7−O$_i^{\prime\prime}$, 8−Ti$_i^{\cdot\cdot\cdot\cdot}$, 9−V$_{Ti}^{\prime\prime\prime\prime}$, 10−V$_{Ti}^{\prime\prime\prime}$, 11−V$_O^X$, 12−0.69 eV.

Fluence, 10^{16} cm^{-2}	m−240	n−160	n−80	n−60
F$_{0.5}$	46	30	32.22	51.5
F$_1$	51.77	39.28	42.76	56.43
F$_2$	56.40	43.56	46.99	62

Table 2. The dependence of integral area of absorption bands in the spectra of TiO$_2$ powders on electron fluence.

powders, the negatively charged defects V_{Ti}'''', V_{Ti}''', and V_O^X are formed, mostly, in the near-IR range, and then positively charged defects $Ti_i^{\cdots}$, $V_O^{\cdot\cdot}$, O_i'', $Ti_i^{\cdots\cdot}$ in the visible and $Ti_i^{\cdot}$, O_i', $V_O^{\cdot}$, and $Ti_i^{\cdot\cdot}$ in the UV ranges are formed.

The analysis of the integral area of the bands during a variety of fluences of electron exposure with energy of 30 keV shows (**Table 2**) that the highest radiation stability belongs to powders with 80–160 nm particle size and the powders with 60 nm particle size possess the lowest radiation stability. Advantageously, the difference is due to a greater concentration of defects V_{Ti}'''', V_{Ti}''', and V_O^X, as well as due to $Ti_i^{\cdots}$ and $V_O^{\cdot\cdot}$ formed defects, which lead to absorption band generation close to 2.17 eV in difference diffuse reflection spectra. The similar band is registered in the spectrum of n−80 nanopowder, but its intensity is significantly less than n−60.

Elementary processes leading to formation and accumulation of such defects are described by reactions given below, where the following designations were accepted: Ti_{Ti}^X, O_O^X, $(Ti_{Ti}^X)^*$, $(O_O^X)^*$—titanium and oxygen atoms and ions in points of lattice; $(H^{\cdot})^*$, $H^{\cdot}$, $(e')^*$, e'—accelerated and thermolyzed proton and electron, correspondingly; $Ti_i^{\cdots\cdot}$, $Ti_i^{\cdots}$, $Ti_i^{\cdot\cdot}$, $Ti_i^{\cdot}$, V_{Ti}'''', V_{Ti}''', V_{Ti}'', V_{Ti}', O_i'', O_i', $V_O^{\cdot\cdot}$, $V_O^{\cdot}$—interstitial ions and vacancies of titanium and oxygen in various charge states; and $h^{\cdot}$—hole. The impact of accelerated electrons leads to interstitial titanium and oxygen generation and corresponding vacancies due to ionizing displacement mechanisms, electrical repulsion from the same charged ions placed close to each other, or the displacement of neighboring simultaneously ionized atoms by the following reactions:

$$Ti_{Ti}X + O_O^X + (e')^* \rightarrow V_{Ti}'''' + Ti_i^{\cdots\cdot} + O_O^X + e' \leftrightarrow V_{Ti}'''' + Ti_i^{\cdots} + O_O^X \tag{5}$$

$$V_{Ti}'''' + Ti_i^{\cdots} \leftrightarrow V_{Ti}''' + Ti_i^{\cdot\cdot} \leftrightarrow V_{Ti}'' + Ti_i^{\cdot} \tag{6}$$

$$Ti_{Ti}^X + O_O^X + (e')^* \rightarrow Ti_{Ti}^X + V_O^{\cdot\cdot} + O_i'' + e' \leftrightarrow Ti_{Ti}^X + V_O^{\cdot} + O_i'' \tag{7}$$

$$V_O^{\cdot} + O_i'' \leftrightarrow V_O^X + O_i' \tag{8}$$
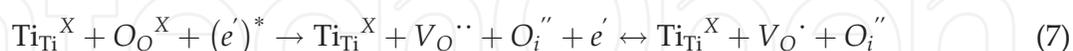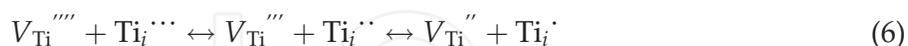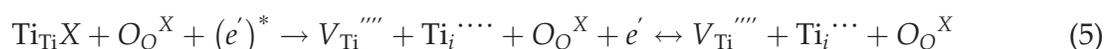
4. Optical properties and radiation stability of titanium dioxide powders after heating and modification with nanoparticles

4.1. Reflection spectra of modified powders

The rutile titanium dioxide pigment (m−240) was used for investigation of an influence of nanoparticle type of various oxide compounds on diffuse reflection spectra of modified TiO$_2$ powder and their changes after accelerated electron irradiation [25]. The average grain size of

nanoparticles was, nm: Al_2O_3—30, ZrO_2—30, ZnO—50, MgO—60, SiO_2—55, and TiO_2—60. The specific surface area of the powders was equal to m^2/g: Al_2O_3—49, ZrO_2—25, ZnO—20, MgO—26, SiO_2—60, and TiO_2—26. All nanopowders possess a crystalline structure except the SiO_2 powder, which was amorphous.

Modification effects on ρ_λ spectra are shown in **Figure 4**. In the range of 440 nm, the reflectivity of heated and modified powders increases by 2–3% (**Figure 5**). An exception is a powder modified with n-ZnO, the ρ value of which reduces by 2–4%. In the range of 580 nm, the reflectivity increases for powders doped by n-MgO and n-TiO_2 only. For other modified powders, the reflectivity does not change noticeably, for the powder doped with ZnO nanoparticles—it decreases as well.

The ρ value of powders modified with n-TiO_2 and n-SiO_2 increases noticeably in the near-IR range at 850 nm. For other modified and heated powders, the ρ changes insignificantly. The increase in ρ is detected in the spectra of powders modified with n-MgO, n-ZrO_2, n-ZnO, and n-SiO_2 at 1200 nm. The largest increase is 4%. The increase in ρ in the range of 1800 nm is observed at both heating and modification by all nanopowders. The largest value, equaled to 4.7%, belongs to powder modified with n-ZnO.

The change in ρ_λ spectra of powders at heating and high-temperature modification can be because of the distinction between the reflection coefficient of nanoparticles and the reflection coefficient of micropowder. This distinction is determined by large value of nanoparticle scattering coefficient in comparison to micro-sized particles and will appear, mainly, in the visible range of spectra.
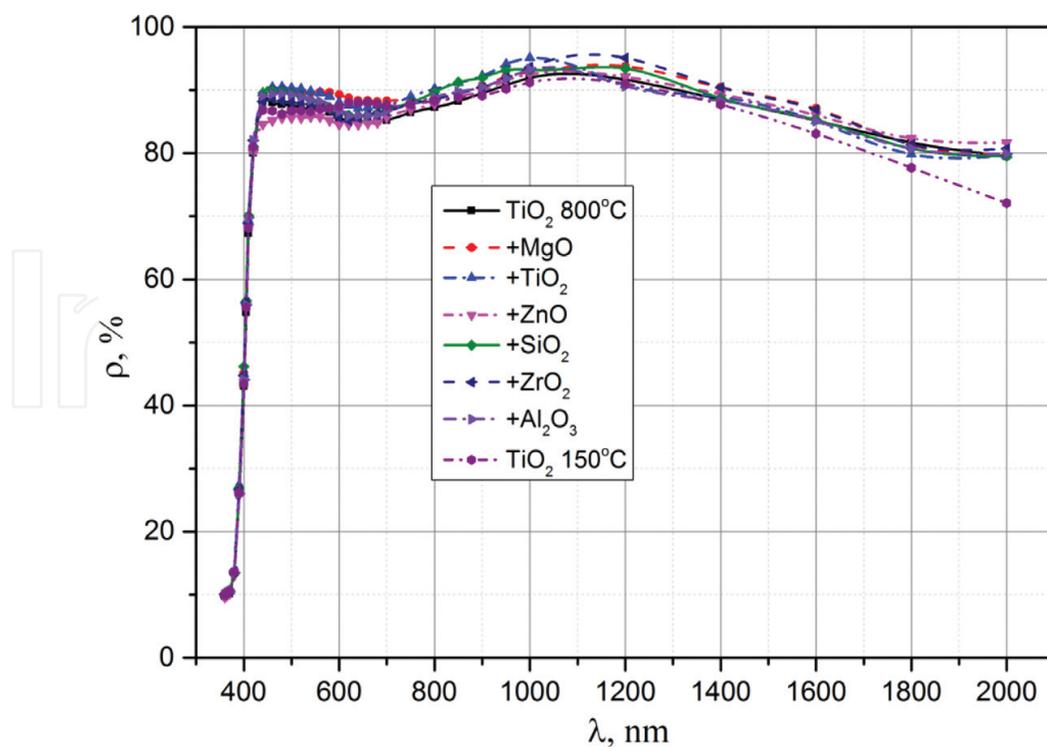
Figure 4. The diffuse reflection spectra of heated at 150 and 800°C unmodified TiO_2 powder and modified with nanoparticles of various oxide compounds in quantity of 7 mass% at 800°C.
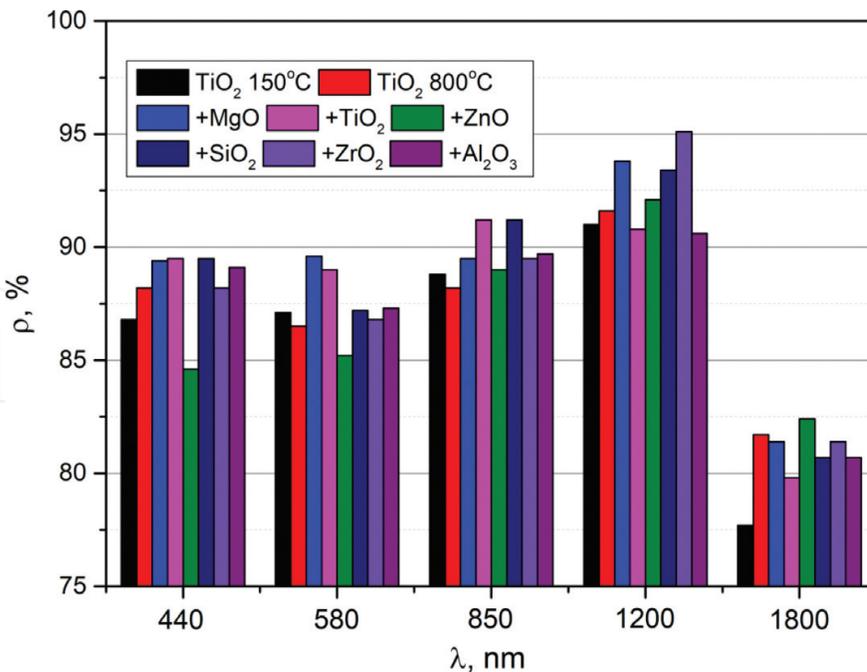
Figure 5. The value of reflection coefficient of unmodified TiO$_2$ powders and modified with nanoparticle of various oxide compounds.

Another reason of the reflection coefficient distinction is desorption of gases molecules from the surface at heating, the main component of which is OH-groups and molecules of water [24, 26]. The desorption leads to a reduction of absorption band intensity in the near-IR range at 1240, 1420, 1950, and 2250 nm [27–29].

An oxygen chemisorption, simultaneously with desorption, on the freed bonds on the surface and oxygen diffusion into the bulk of powder grains occur at heating in atmosphere. This leads to a decrease in the concentration of native point defects, to a decrease in the intensity of the absorption bands, and to an increase in the reflection coefficient in the regions where the bands are located.

4.2. Radiation stability of modified powders

Radiation stability was estimated from the difference diffuse reflection spectra ($\Delta\rho_\lambda$), in which two parts can be distinguished, determined by the absorption bands. In the visible range the bands at 420–580 nm are registered, in the near-IR range at 850–1200 nm (**Figure 6**). The position of maximums changes depending on type of nanopowder. Two bands appear in some spectra and one band in others. Based on types and number of absorption bands in these ranges of TiO$_2$ absorption spectra, it can be assumed that these integral contours include a large number of elementary bands. The $\Delta\rho$ values in these regions are different: for some powders, they are approximately the same; for others, the intensity of the band in the near-IR region is substantially larger.

Judging by the $\Delta\rho_\lambda$ values, it can be concluded that the largest changes occur during irradiation in the visible range in the powder heated at 150°C and in the powders modified with n-MgO and n-ZnO. The changes in ρ_λ spectra reach 27% after exposure.
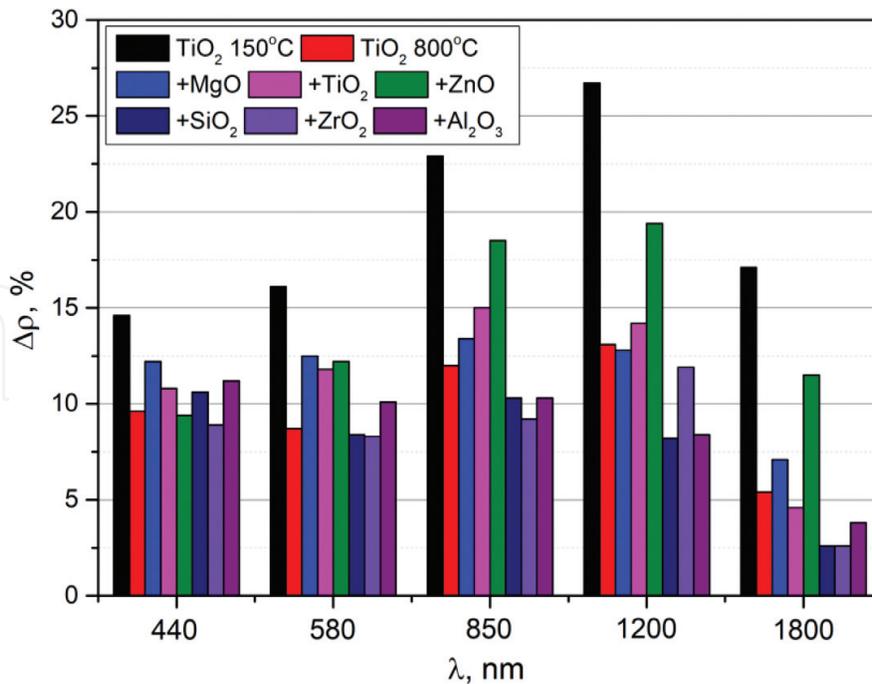
Figure 6. The $\Delta\rho$ values of heated and modified TiO_2 powders by nanoparticles of different oxide compounds for various wavelengths.

The radiation stability of TiO_2 powders modified by all types of nanoparticles is higher compared to unmodified powder but heated at 150°C. A reduction in $\Delta\rho$ values of modified powders is registered in entire range of $\Delta\rho_\lambda$ spectra (**Figure 6**). The effectiveness of modification ($\Delta\rho_{150}/\Delta\rho_{mod}$) reaches almost two times in the visible range. In the near-IR range, it is even larger and reaches more than six times. The best result in the visible range corresponds to n-ZrO_2 modification, in the near-IR range—n-SiO_2.

Radiation stability in the visible region of the spectrum of TiO_2 powder heated at 800°C is the same or even higher in comparison to the modified powders. Only the modification with n-ZrO_2 gives, although not significant, an increase in radiation stability compared to the heated powder. Modification with n-SiO_2 nanopowder results in a slight decrease and the modification with n-MgO, n-ZnO, n-Al_2O_3, and n-TiO_2 to a noticeable decrease in radiation stability in comparison to the heated powder.

In the near-IR region, the modification with some nanopowders has a significant effect on the radiation stability. The largest effect was obtained using n-SiO_2 and n-ZrO_2. Then, mixtures with n-Al_2O_3 and n-TiO_2 follow. The least effect from the modification was obtained using n-MgO and n-ZnO.

With respect to the aggregate values of $\Delta\rho$ in the visible and near-IR regions of the spectrum, the series of the largest effect at modifying with nanoparticles is as follows: 1—SiO_2, 2—ZrO_2, 3—Al_2O_3, 4—TiO_2, 5—MgO, and 6—ZnO. The largest effect in increasing the radiation stability of micropowders of titanium dioxide is obtained by modifying with n-SiO_2 and n-ZrO_2 and the smallest by the modification with n-MgO and n-ZnO.

4.3. The effect of temperature at heating and modification by SiO$_2$ nanoparticles on the radiation stability of TiO$_2$ powders

A comparison of the ρ_λ spectra of heated TiO$_2$ powders shows (**Figure 7**) that with an increase in the heating temperature from 150 to 400°C, the reflection coefficient varies in different regions of the spectrum according to various regularities [26]. In the region from the absorption edge up to 600 nm, it increases so that an absorption band with a maximum at 400–405 nm is formed in the difference spectrum determined by the relation:

$$\Delta\rho_\lambda = \rho_{\lambda 150} - \rho_{\lambda 400} \tag{9}$$

where $\rho_{\lambda 150}$ and $\rho_{\lambda 400}$ are the reflection coefficients of the powder heated at a temperature of 150 and 400°C, respectively.

In the 600–900 nm region, the reflection coefficient slightly decreases with a minimum value of 1.7% at 700 nm. In the longer wavelength region, it increases in accordance with power law of the wavelength [30, 31].

An increase in the heating temperature up to 800°C leads to the appearance of an absorption band at 380–390 nm in the difference spectrum ($\Delta\rho_\lambda = \rho_{\lambda 150} - \rho_{\lambda 800}$). At 450–680 nm, the changes are close to zero, and in the region of 680–2100 nm, a power function of the wavelength with a maximum value $\Delta\rho = 8.7\%$ is recorded.

Modification of the TiO$_2$ powder with SiO$_2$ nanoparticles and heating at 400°C, both lead to a decrease in the reflection coefficient over the entire spectrum (**Figure 8**). At the same time, an absorption band is recorded in the region from the absorption edge up to 600 nm with a maximum at 500 nm, and in the longer wavelength region, the reflection coefficient changes without certain regularities, the $\Delta\rho$ values are 2–3%.

An increase in the heating temperature up to 800°C at modifying TiO$_2$ powder leads to a decrease in the reflection coefficient in the region from the absorption edge up to 600 nm and
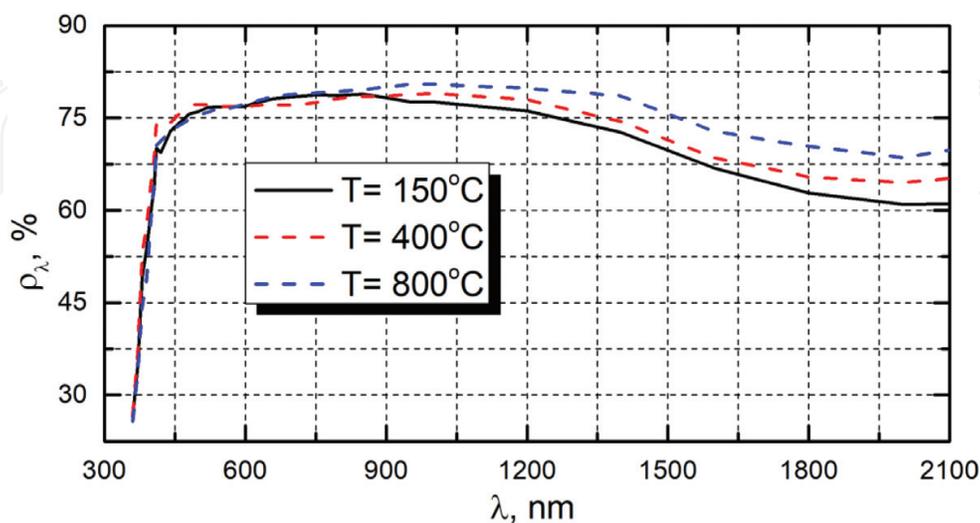

Figure 7. The diffuse reflection spectra of unmodified titanium dioxide powders heated at various temperatures.
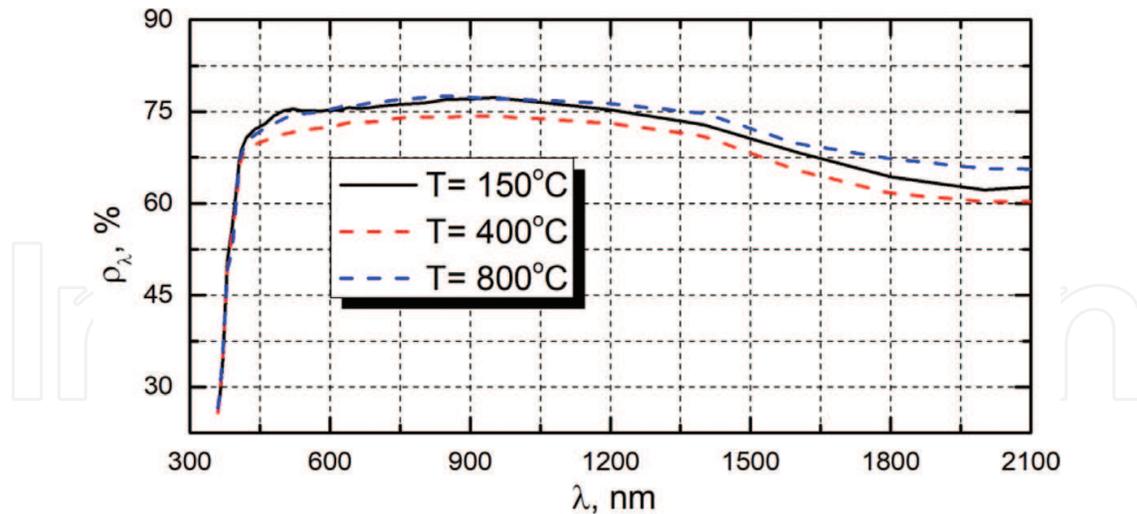
Figure 8. Diffuse reflection spectra of TiO$_2$ powders heated at different temperatures and modified with SiO$_2$ nanopowders.

its increase in the longer wavelength region. The $\Delta\rho$ values are no more than 1% except for two regions: the bands with a maximum at 400–405 nm and the "tail" of absorption in the range of 900–2100 nm reaching 3.5% and 3.7%, respectively.

Analysis of the ρ_λ spectra of heated and modified by nanoparticles at different temperatures of titanium dioxide powders shows that the change in the reflection coefficient in the entire spectral region is determined by several processes, which lead to the appearance of qualitatively different dependences. A band with a maximum at 400–500 nm caused by defects of cationic sublattice (interstitial ions or absorption vacancies) is on the first region in the range from the absorption edge to 600 nm of TiO$_2$. The range from 680 or 900 nm to 2100 nm is the second region and can be described by a power-law dependence of the absorption coefficient from the wavelength because of electron transitions between levels in the conduction band of TiO$_2$. In the interval between these two regions, the difference values of the reflection coefficient change insignificantly or form an absorption band with a maximum at 700 nm.

Therefore, heating the TiO$_2$ powder at 400 and 800°C without nanoparticles and in mixtures with SiO$_2$ nanoparticles leads to a change in the concentration of native point defects and free electrons on the surface. Such changes are determined by the desorption of physically and chemically sorbed gases, the release of bonds, their filling with other molecules and atoms, i.e., redistribution of defects and electronic state on the surface.

Exposure with electrons leads to a decrease in the reflection coefficient over the entire spectrum as a result of the formation of radiation defects and the appearance of the absorption bands induced by them. With an increase in the heating temperature from 150 to 400°C, very slight changes in the absorption coefficient occur (**Figure 9**).

Since the heating at 150°C does not give noticeable changes in the absorption coefficient a_s, then the Δa_s values of the heated powder at 150°C are taken as the values of the initial (unheated) powder, and the efficiency of the TiO$_2$ micropowder modification by the SiO$_2$ nanopowder in an amount of 7 mass% at a temperature of 400 or 800° C was computed as follows:

$$\eta = \Delta a_s^{150} / \Delta a_s^{T} \tag{10}$$

where Δa_s values after irradiation with 0.5, 1, and 2×10^{16} cm^{-2} electron fluence: $\Delta a_s^{150} - \text{TiO}_2$ powders heated at 150°C, Δa_s^{T} are the Δa_s values of TiO$_2$ powder modified with 7 mass% of SiO$_2$ nanoparticles at a temperature of 400 or 800°C.

With an increase in the electron fluence from F = 1×10^{16} cm^{-2} to F = 2×10^{16} cm^{-2}, the coefficient η varies insignificantly for all values of the heating and modifying temperature (**Figure 10**) in comparison to its changes in the range of F = $(0.5–1) \times 10^{16}$ cm^{-2}. This allows us to assume that the values obtained at F = 2×10^{16} cm^{-2} are close to the steady-state values.

The decrease in the efficiency of silica nanopowder modification with increasing exposure time or electron fluence is, probably, determined by the contribution of the surface preradiation defects in the total concentration of radiation defects formed by irradiation both in the TiO$_2$ micropowder and in SiO$_2$ nanoparticles.

When the electron fluence is less than 0.5×10^{16} cm^{-2}, the main contribution to the change in the diffuse reflection spectra and the integral absorption coefficient is made by preradiation defects on the grain surface of the crystal lattice of the TiO$_2$ powder.

Upon irradiation by accelerated electrons with prethreshold energies (e*), the processes of formation and separation of charge carriers in titanium dioxide proceed according to the scheme:

a. Hole-electron formation

$$\text{TiO}_2 + e^* \rightarrow e^- + p^+ \tag{11}$$

b. Hole drift toward negatively charged surface, then an interaction with sorbed radicals and their oxidation

$$p^+ + R \rightarrow \text{RO}^- \tag{12}$$

c. Neutralization of surface oxygen by holes

$$p^+ + O_s(O_l) \rightarrow O \tag{13}$$

d. Oxygen formation and its escape in vacuum

$$O + O \rightarrow O_2\uparrow \tag{14}$$

Holes move to the surface, where they first interact with surface oxygen, then with the oxygen of the lattice that leads to its radiolysis. If there are defects on the surface, then holes relax on these defects and SiO$_2$ nanoparticles do not play a special role in increasing the radiation stability. And only at an optimal value of the nanoparticle concentration which is sufficient to create the necessary number of relaxation centers along with the available native surface defects—native relaxation centers, the modification becomes effective.

Based on the results of studies of the temperature effect on optical properties (**Figures 9** and **10**) at the TiO$_2$ powders heating and their modification by SiO$_2$ nanoparticles, the following can be concluded:

1. Heating at 400°C does not give a noticeable increase in optical properties stability during electron exposure in comparison with the heating at 150°C. The increase is significant for modified powders, and the coefficient η is 2.38, 1.8, and 1.73 for electron fluence (0.5, 1, and 2) $\times 10^{16}$ cm^{-2}, respectively.

2. Heating at 800°C leads to an increase in the radiation stability of both types of powders. In this case, the coefficient η is 1.82, 1.48, and 1.43 for unmodified and 2.65, 2.31, and 2.26 for modified powders for electron fluence (0.5, 1, and 2) $\times 10^{16}$ cm^{-2}, respectively.

3. A comparison of these values shows that, with respect to the coefficient η and its dependence on the electron fluence, the modification at a temperature of 400°C leads to approximately the same effect (η = 2.38, 1.8 and 1.73) as the heating at 800°C (η = 1.82, 1.48, and 1.43). The effectiveness of such a method of processing powders is manifested: modification at a reduced temperature gives the same effect as heating at a higher temperature.

4. The lack of improvement in radiation stability from heating at 400°C can be a consequence of the fact that at such a temperature, the surface of titanium dioxide particles is released only from physically bounded water on the surface and OH^{-} groups. Surface bonds are not released, and there is no chemisorption of oxygen, which does not give noticeable changes in the concentration of anionic sublattice defects.

5. A noticeable improvement in the radiation stability of the powder modified at 400°C testifies to the effect of SiO$_2$ nanoparticles, which are on the surface of grains and granules of titanium dioxide, as centers of relaxation of electronic excitations arise upon irradiation. This effect is more pronounced at low electron fluences (η = 2.38 at F = 0.5 $\times 10^{16}$ cm^{-2}), i.e., when the surface preradiation defects in titanium dioxide determine a degradation. At such a temperature and electron fluence of 0.5 $\times 10^{16}$ and 1 $\times 10^{16}$, these defects, basically, transform to color centers. This is evidenced by the almost complete equality of the absorption coefficient at an increase in the heating temperature from 400–800°C: Δa_s = 0.029 for T = 400°C and Δa_s = 0.026 for T = 800°C. From this point, the following can be concluded that in the case of small values of the electron fluence (or absorbed dose), a rather low heating temperature (400°C) is sufficient at modification with nanoparticles.

6. If the electron fluence increases to (1–2) $\times 10^{16}$ cm^{-2}, then the change in Δa_s values of specimens heated at 400 and 800°C increases from 0.03 up to 0.1 and 0.13, respectively. This means that for large values of fluence, the SiO$_2$ nanoparticles on the surface of TiO$_2$ grains and granules are not sufficient to perform the function of relaxation centers of electronic excitations. Therefore, in order to clean the surface from chemosorbed gases, the appropriate conditions, such as heating at 800°C, should be provided.

The fact that the radiation stability at the same heating temperature is higher in mixtures of TiO$_2$ + SiO$_2$ powders than TiO$_2$ powders may indicate about a change in the catalytic activity, specific surface area, and concentration of chemisorbed gases upon the addition of SiO$_2$ nanoparticles. The reduction in the catalytic activity which depends on the anionic vacancy concentration and excess titanium on the surface [32] will occur at heating in an atmosphere with a large oxygen concentration. Such a heating, in turn, will lead to an increase in radiation stability.
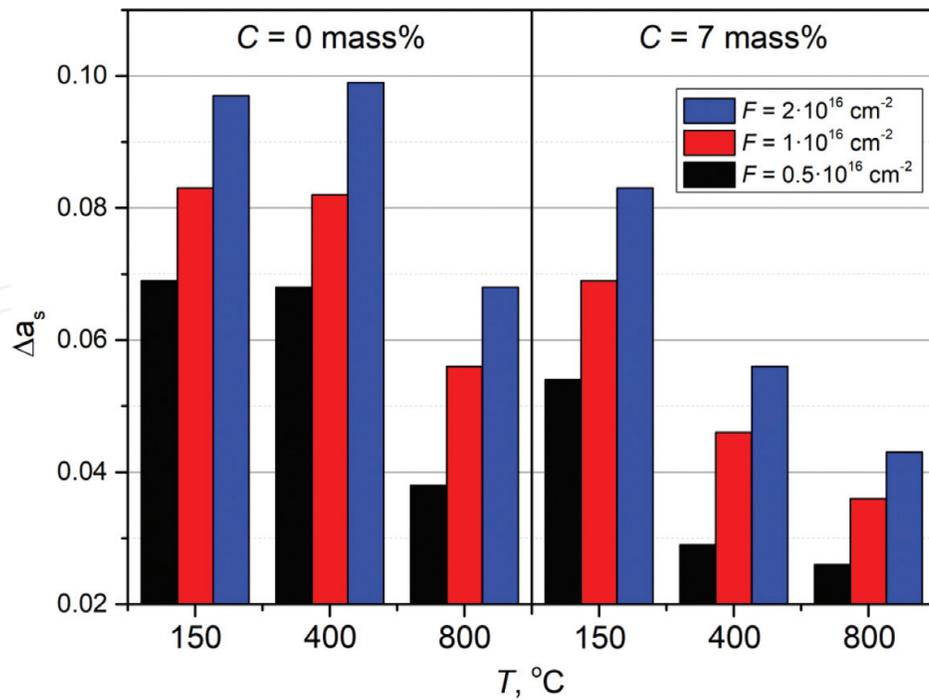
Figure 9. Dependence of Δa_s values on the electron fluence with 30 keV energy of TiO$_2$ powder heated at the temperature of 150, 400, and 800°C and modified with SiO$_2$ nanoparticles in an amount of 7 mass% by heating at the same temperature values.
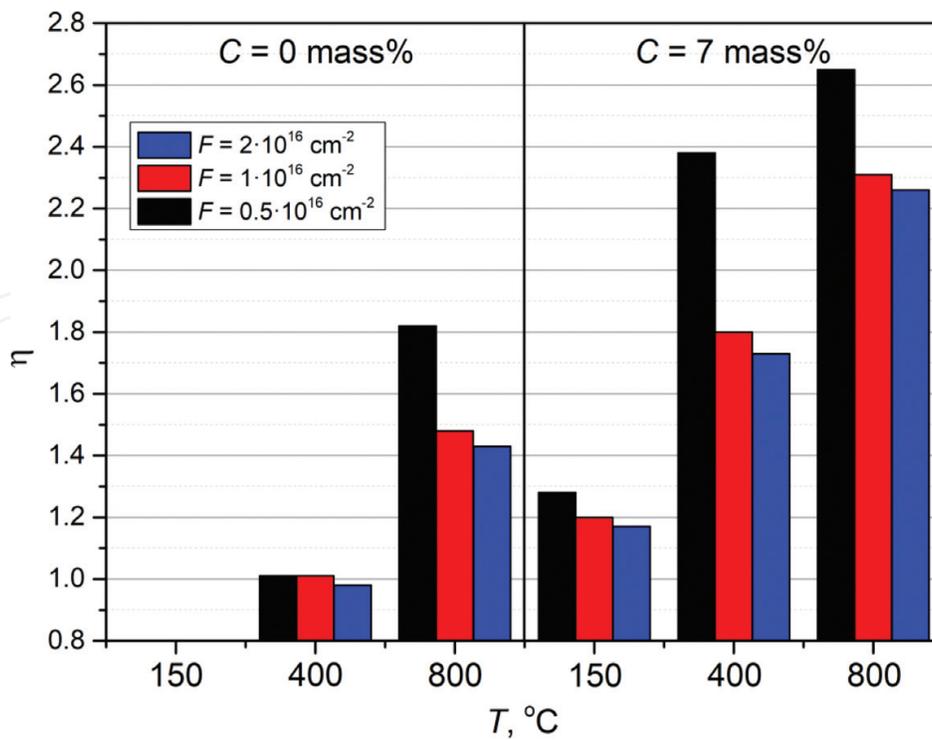
Figure 10. Effectiveness of the heating and TiO$_2$ powder modification (η) with SiO$_2$ nanoparticles.
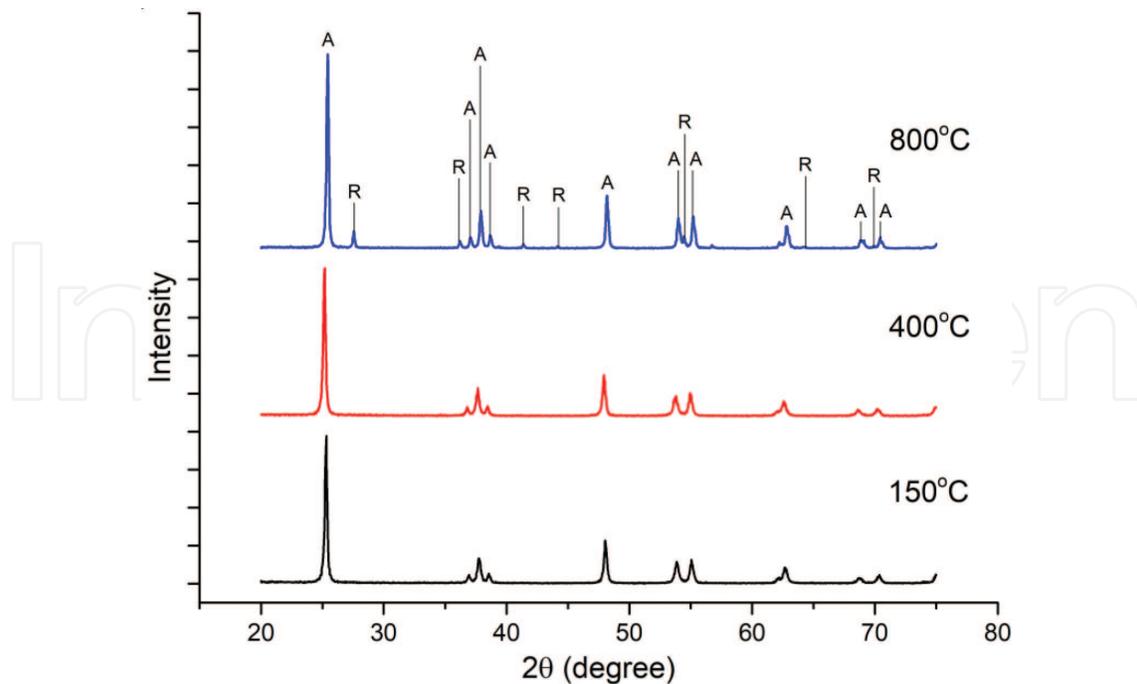
Figure 11. X-ray diffraction patterns of TiO_2 powders modified with SiO_2 nanoparticles at a variety of heating temperatures.

The heating of TiO_2 powder mixtures with SiO_2 nanoparticles at a temperature of 150, 400, and 800°C cannot lead to the formation of new phases, because even at a higher heating temperature (900, 1000, and 1200°C) of TiO_2 + SiO_2 powder mixtures, the $Ti_{(1-x)}Si_xO_2$ solid solution is not formed [33].

A certain contribution to the increase in radiation stability at the highest heating temperature in the present studies, equaled to 800°C, can be made by changing the phase state of TO_2 powder—the conversion of anatase to rutile, which is carried out at a temperature of 450–900°C. The transition temperature is determined by the degree of crystallinity of the compound (films, polycrystals, and single crystals), the concentration of defects, and other factors [34, 35].

When SiO_2 particles are added to the TiO_2 powder, the phase transition is facilitated: transition temperature reduces and the relative rutile concentration increases [33]. Therefore, the TiO_2 powder mixtures with SiO_2 nanoparticles heated at 800°C can give an increase in the relative rutile concentration, a change in the particle size and specific surface area, the concentration of absorbed gases, and stability to an impact of electron exposure. A confirmation of the increase in rutile concentration with increasing temperature is the results of X-ray phase analysis (**Figure 11**), which show that an increase in the heating temperature from 150–400°C does not change the phase ratio, and further increase to 800°C leads to the formation of rutile in an amount 10 mass%.

5. Conclusions

In this chapter, the optical properties and radiation stability of titanium dioxide powders before and after modification by nanopowders of various oxide compounds (Al_2O_3, ZrO_2, SiO_2, TiO_2, ZnO, and MgO) are considered.

The reflectivity of modified powders can both increase, in comparison to the initial powders, and decrease. The reflection coefficient is determined by the grain sizes and, with their decrease, it increases, which occurs when nanopowders are added. The decrease in the reflection coefficient may be due to a large absorption by native point defects in the UV and visible ranges and by chemisorbed gases in the near-IR range of the spectrum, determined by the larger specific surface area of nanopowders.

Modification with nanopowders leads to an increase in the radiation stability of reflective powders, which is determined by the relaxation of electronic excitations on the surface of nanoparticles and by a smaller concentration of absorption centers formed upon irradiation. The maximum effect of increasing radiation stability is achieved by modification by nanopowders with a larger specific surface area and a smaller particle size. An additional factor affecting the increase in radiation stability is the heating during the modification, and the largest effect was obtained at T = 800°C.

Acknowledgements

Author details

Mikhail M. Mikhailov[1], Vitaly V. Neshchimenko[1,2], Semyon A. Yuryev[1]* and
Alexey N. Sokolovskiy[3]

*Address all correspondence to: yusalek@gmail.com

1 Radiation and Space Materials Laboratory, Tomsk State University of Control Systems and Radio-electronics, Tomsk, Russia

2 Space Materials Laboratory, Amur State University, Blagoveshchensk, Russia

3 University of Washington, Seattle, USA

References

[1] Ma Y, Wang X, Jia Y, Chen X, Han H, Li C. Titanium dioxide-based Nanomaterials for Photocatalytic fuel generations. Chemical Reviews. 2014;**114**(19):9987-10043. DOI: 10.1021/cr500008u

[2] Akpan UG, Hameed BH. Parameters affecting the photocatalytic degradation of dyes using TiO2-based photocatalysts: A review. Journal of Hazardous Materials. 2009;**170**(2–3): 520-529. DOI: 10.1016/j.jhazmat.2009.05.039

[3] Chihiro I, Iwahashi K, Kan'no K. Photogeneration of charge carriers in titanium oxides. Nuclear Instruments and Methods in Physics Research Section B: Beam Interactions with Materials and Atoms. 2002;**191**(1–4):271-274. DOI: 10.1016/S0168-583X(02)00574-8

[4] Zhang L. Chen Rong-min. TiO2-Siloxane thermal control coatings for protection of space-craft polymers. Chinese Journal of Aeronautics. 2004;**17**(1):53-59. DOI: 10.1016/S1000-9361(11)60203-3

[5] Dobrzański LA, Szindler M. Sol gel TiO2 antireflection coatings for silicon solar cells. Journal of Achievements in Materials and Manufacturing Engineering. 2012:**52**(1):7-14

[6] Baraton M-I. Nano-TiO2 for solar cells and Photocatalytic water splitting: Scientific and technological challenges for commercialization. The Open Nanoscience Journal. 2011;**5**: 64-77. DOI: 10.2174/1874140101105010064

[7] Khan MA, Khan SMM, Mohammed MA, Sultana S, Islam JMM, Uddin J. Sensitization of Nanocrystalline titanium dioxide solar cells using natural dyes: Influence of acids medium on coating formulation. American Academic & Scholarly Research Journal. 2012;**4**(5)

[8] Chen X, Mao SS. Titanium dioxide nanomaterials: Synthesis, properties, modifications and applications. Chemical Reviews. 2007;**107**(7):2891-2959. DOI: 10.1021/cr0500535

[9] Mikhailov MM, Utebekov TA, Neshchimenko VV. Radiation stability of powders in mixtures with Al2O3 nanoparticles. Radiation Effects and Defects in Solids. 2013;**168**(2): 106-114. DOI: 10.1080/10420150.2012.693084

[10] Mikhailov MM, Verevkin AS. Optical properties and radiation stability of thermal control coatings based on doped zirconium dioxide powders. Journal of Materials Research. 2004;**19**(2):535-541. DOI: 10.1557/jmr.2004.19.2.535

[11] Li XW, Song RG, Jiang Y, Wang C, Jiang D. Surface modification of TiO_2 nanoparticles and its effect on the properties of fluoropolymer/TiO_2 nanocomposite coatings. Applied Surface Science. 2013;**276**:761-768. DOI: 10.1016/j.apsusc.2013.03.167

[12] Mikhailov MM, Lapin AN. Influence of the temperature of aluminum oxide micropowder modification with Al2O3 nanopowders on the optical properties and radiation resistance of coatings manufactured on their basis. Russian Physics Journal. 2011;**53**(11):1131-1139. DOI: 10.1007/s11182-011-9541-3

[13] Mikhailov MM, Neshchimenko VV, Li C. The degradation kinetics of the optical properties under proton irradiation for ZnO pigments modified by Al2O3 and Al2O3·CeO2 nanopowders. Radiation Effects and Defects in Solids. 2012;**167**(1):26-36. DOI: 10.1080/10420150.2011.588231

[14] Mikhailov MM, Neshchimenko VV, Li C. Radiation stability of zinc oxide pigment modified by zirconium oxide and Aluminum oxide Nanopowders. AIP Conf. Proc. 2009:680-690. DOI: 10.1063/1.3076886

[15] Kositsyn LG, Mikhailov MM, Kuznetsov NY, Dvoretskii MI. Apparatus for study of diffuse – Reflection and luminescence spectra of solids in vacuum. Instruments and Experimental Techniques. 1985;**28**:929-932

[16] Johnson FS. The solar constant. Journal of Meteorology. 1954;**11**(6):431-439. DOI: 10.1175/ 1520-0469(1954)011<0431:TSC>2.0.CO;2

[17] Mikhailov MM, Neshchimenko VV, Yuryev SA. Optical properties and radiation stability of submicro- and nanopowders titanium dioxide measured in situ. Radiation Physics and Chemistry. 2016;**121**:10-15. DOI: 10.1016/j.radphyschem.2015.12.006

[18] Pidgeon CR. In: Balkanski M, eds. Handbook on Semiconductors. North Holland: Amsterdam. 1980

[19] He J, Behera RK, Finnis MW, Li X, Dickey EC, Phillpot SR, Sinnott SB. Prediction of high-temperature point defect formation in TiO2 from combined ab initio and thermodynamic calculations. ActaMater. 2007;**55**:4325-4337. DOI: 10.1016/j.actamat.2007.04.005

[20] Chen J, Lin L-B, Jing F-Q. Theoretical study of F-type color center in rutile TiO2. Journal of Physics and Chemistry of Solids. 2001;**62**:1257-1262. DOI: 10.1016/S0022-3697(01)00018-X

[21] Seebauer Edmund G, Kratzer MC. Charged point defects in semiconductors. Materials Science and Engineering R. 2006;**55**:57-149. DOI: 10.1016/j.mser.2006.01.002

[22] Nakamura I, Negishi N, Kutsuna S, Ihara T, Sugihara S, Takeuchi K. Role of oxygen vacancy in the plasma-treated TiO2 photocatalyst with visible light activity for NO removal. Journal of Molecular Catalysis A: Chemical. 2000;**161**:205-212. DOI: 10.1016/ S1381-1169(00)00362-9

[23] Kuznetsov VN, Serpone N. On the origin of the spectral bands in the visible absorption spectra of visible-light-active TiO2 specimens. Analysis and assignments. Journal of Physical Chemistry C. 2009;**113**:15110-15123. DOI: 10.1021/jp901034t

[24] Mikhailov MM, Chundong L, Neshchimenko VV. Optical property degradation of titanium dioxide micro- and nanopowders under irradiation. Nuclear Instruments and Methods in Physics Research Section B: Beam Interactions with Materials and Atoms. 2014;**333**:52-57. DOI: 10.1016/j.nimb.2014.04.014

[25] Mikhailov MM, Vlasov VA, Yuryev SA, Neshchimenko VV, Shcherbina VV. Optical properties and radiation stability of TiO2 powders modified by Al2O3, ZrO2, SiO2, TiO2, ZnO, and MgO nanoparticles. Dyes and Pigments. 2015;**123**:72-77. DOI: 10.1016/j. dyepig.2015.07.024

[26] Mikhailov MM, Yuryev SA, Remnev GE, Sazonov RV, Kholodnaya GE, Ponomarev DV. Effect of temperature on radiation resistance of TiO$_2$ powders during heating and modification by SiO$_2$ nanoparticles. Nuclear Instruments and Methods in Physics Research Section B: Beam Interactions with Materials and Atoms. 2014;**336**:96-101. DOI: 10.1016/j. nimb.2014.07.002

[27] Blanco M, Coello J, Ityrriaga H, Maspoch S. Near-infrared spectroscopy in the pharmaceutical industry. The Analyst. 1998;**123**:135-150. DOI: 10.1039/A802531B

[28] Blanco M, Vilarroya I. NIR spectroscopy: A rapid-response analytical tool. Trac trends in Analytical Chemistry. 2002;**21**:240-250. DOI: 10.1016/S0165-9936(02)00404-1

[29] Mikhailov MM, Neshchimenko VV, Li C. Effect of the heat treatment on reflective Spectrum of the zinc oxide powders. Journal of Materials Research. 2009;**24**(1):19-23. DOI: 10.1557/JMR.2009.0033

[30] Hunsperger RG. Integrated Optics: Theory and Technology. Springer; 2009. 513 p. DOI: 10.1007/b98730

[31] Peter YU, Cardona M. Fundamentals of Semiconductors: Physics and Materials Properties. Springer; 2010. 778 p. DOI: 10.1007/978-3-642-00710-1

[32] Mitsuhara K, Matsuda T, Okumura H, Visikovskiy A, Kido Y. Oxygen deficiency and excess of rutile titania (1 1 0) surfaces analyzed by ion scattering coupled with elastic recoil detection. Nuclear Instruments and Methods in Physics Research Section B: Beam Interactions with Materials and Atoms. 2011;**269**(16):1859-1864. DOI: 10.1016/j.nimb.2011.05.007

[33] Tobaldi DM, Tucci A, Škapin AS, Esposito L. Effects of SiO_2 addition on TiO_2 crystal structure and photocatalytic activity. Journal of the European Ceramic Society. 2010; **30**(12):2481-2490. DOI: 10.1016/j.jeurceramsoc.2010.05.014

[34] Nowotny J. Titanium dioxide-based semiconductors for solar-driven environmentally friendly applications: Impact of point defects on performance. Energy & Environmental Science. 2008;**1**:565-572. DOI: 10.1039/B809111K

[35] Lu Z, Jiang X, Zhou B, Wu X, Lu L. Study of effect annealing temperature on the structure, morphology and photocatalytic activity of Si doped TiO_2 thin films deposited by electron beam evaporation. Applied Surface Science. 2011;**257**(24):10715-10720. DOI: 10.1016/j.apsusc.2011.07.085